

Delayed Minimally Invasive Injection of Allogenic Bone Marrow Stromal Cell Sheets Regenerates Large Bone Defects in an Ovine Preclinical Animal Model

ARNE BERNER,^{a,b,*} JAN HENKEL,^{a,*} MARIA A. WOODRUFF,^a ROLAND STECK,^{a,c} MICHAEL NERLICH,^b MICHAEL A. SCHUETZ,^a DIETMAR W. HUTMACHER^a

Key Words. Large bone defect • Mesenchymal stem cells • Allogenic • Bone tissue engineering • Cell injection • Bone regeneration • Sheep

ABSTRACT

Cell-based tissue engineering approaches are promising strategies in the field of regenerative medicine. However, the mode of cell delivery is still a concern and needs to be significantly improved. Scaffolds and/or matrices loaded with cells are often transplanted into a bone defect immediately after the defect has been created. At this point, the nutrient and oxygen supply is low and the inflammatory cascade is incited, thus creating a highly unfavorable microenvironment for transplanted cells to survive and participate in the regeneration process. We therefore developed a unique treatment concept using the delayed injection of allogenic bone marrow stromal cell (BMSC) sheets to regenerate a critical-sized tibial defect in sheep to study the effect of the cells' regeneration potential when introduced at a postinflammatory stage. Minimally invasive percutaneous injection of allogenic BMSCs into biodegradable composite scaffolds 4 weeks after the defect surgery led to significantly improved bone regeneration compared with preseeded scaffold/cell constructs and scaffold-only groups. Biomechanical testing and microcomputed tomography showed comparable results to the clinical reference standard (i.e., an autologous bone graft). To our knowledge, we are the first to show in a validated preclinical large animal model that delayed allogenic cell transplantation can provide applicable clinical treatment alternatives for challenging bone defects in the future. *STEM CELLS TRANSLATIONAL MEDICINE* 2015;5:1–10

SIGNIFICANCE

From a translational point of view, we present a comprehensive study, the results of which show that percutaneous injection of allogenic BMSCs into the biodegradable composite scaffold 4 weeks after the defect surgery led to significantly improved bone regeneration compared with preseeded scaffold/cell constructs and scaffold-only groups. Biomechanical testing and microcomputed tomography showed results comparable to those of the clinical gold standard, namely autologous autograft. To our knowledge, we are the first to display in a validated preclinical large animal model that delayed allogenic cell transplantation could provide clinical treatment alternatives for challenging bone defects in the future.

INTRODUCTION

The use of autologous and allogenic mesenchymal stem cells (MSCs) has been extensively investigated in numerous fields of regenerative medicine, including cardiovascular disease [1, 2], endocrine disorders such as diabetes [3], wound healing [4], autoimmune disorders [5], neurological conditions such as stroke [6] or multiple sclerosis [7], pulmonary disease [8], solid organ transplantation [9], and musculoskeletal disease [10]. However, the functional role of MSCs in the regeneration of different tissues is not fully understood, and their discussion in published studies is often controversial [11–14].

Despite many relatively successful outcomes of cell-based bone tissue engineering in small animals, the transfer of these concepts into preclinical large animal models and/or routine clinical practice has not yet been realized [15–20]. In bone regeneration research, tissue engineering constructs (TECs) loaded or seeded with cells are often transplanted into a bone defect immediately after the defect has been created. In line with this argument, our previously published studies demonstrated only limited bone regeneration occurring after implantation of preseeded and cultured TECs in a large preclinical animal model [21]. When a defect is created, the nutrient

^aInstitute of Health and Biomedical Innovation and ^cMedical Engineering Research Facility, Queensland University of Technology, Brisbane, Queensland, Australia; ^bDepartment of Trauma Surgery, University of Regensburg, Regensburg, Germany

*Contributed equally.

Correspondence: Dietmar W. Hutmacher, Ph.D., Institute of Health and Biomedical Innovation, Queensland University of Technology, 60 Musk Avenue, Kelvin Grove, Queensland 4059, Australia. Telephone: 617-3138-6077; E-Mail: dietmar.hutmacher@qut.edu.au

Received October 29, 2014; accepted for publication January 28, 2015.

©AlphaMed Press 1066-5099/2015/\$20.00/0

<http://dx.doi.org/10.5966/sctm.2014-0244>

and oxygen supply in the operated tissue is significantly compromised and an inflammatory reaction is usually in progress. Therefore, the introduction of MSCs into a physiologically compromised bone defect microenvironment is associated with a low cell survival rate, resulting in compromised bone regeneration, because the cells are not collectively able to exert a regenerative effect. The stages of bone regeneration during physiological bone defect healing initiate with an inflammatory reaction and progress through to the regenerative phase (soft callus) [22]. The duration of the initial inflammation phase depends on the size and volume of the defect and usually ends after approximately 2–3 weeks. During the inflammation reaction, macrophages and platelets are present in the defect area, but during the soft callus phase, the predominant cell type changes to endothelial cells, MSCs, and chondrocytes [23]. Hence, the physiological environment for the bone marrow stromal cells (BMSCs) to reside in is more akin to the environment present after the inflammation reaction has subsided. Furthermore, an ingrowth of new blood vessels into the defect area occurs in the soft callus phase, resulting in a higher nutrient and oxygen supply in this phase of fracture healing [24].

Based on this information, we developed a unique concept of delayed minimally invasive injection of BMSCs into a preimplanted composite scaffold in a validated critical-sized and preclinical ovine segmental bone defect model. Instead of delivering the cells into the defect site at the time the defect was created, which is the traditional scaffold-based tissue engineering approach, we hypothesized that postponing the cell delivery would have beneficial effects owing to the microenvironment becoming more conducive to cell survival in the later stages of bone healing. This should allow the initial inflammatory reaction to subside and a sufficient oxygen supply in the defect site to develop, thereby creating a more viable environment for the injected cells. We also hypothesized that the technique of delayed injection of allogenic BMSCs would lead to a higher cell survival rate and therefore to increased bone formation, comparable to the new bone formation achieved using autologous bone grafts (ABGs). Therefore, we modified the experimental setup of a classic scaffold cell-based bone engineering strategy using our previously established ovine large segmental bone defect model [25, 26]. We opted to implant the scaffold without cells in a first procedure. Four weeks after the initial defect creation and scaffold implantation, allogenic BMSCs were then injected using a unique minimally invasive percutaneous approach (supplemental online Video 1).

During the past 7 years, our research group has successfully established a world-leading, 3-cm segmental tibial defect ovine animal model at the Queensland University of Technology [26, 27]. The methods used in this animal model are highly standardized, and the mechanical conditions are fully characterized [25]. This enables highly significant comparisons between various tissue engineering applications investigated using this preclinical ovine animal model. By comparing the regenerative capacity of potential novel tissue engineering applications to our well-established control groups (i.e., empty bone defects without any treatment and the clinical reference standard of ABGs), we are able to investigate the potential of novel constructs compared with highly standardized controls (the results for the control groups can be found in [25]).

The aim of the present study was to assess and compare the bone regenerative potential of a novel technique of minimally invasive delayed injection of allogenic BMSCs combined with

a biodegradable composite to the application of ABGs in our well-established critical-sized sheep segmental defect model.

MATERIALS AND METHODS

Surgical Procedure

In 24 male Merino sheep (weight 40–50 kg, age 7–8 years), a critical-sized, 3-cm tibial defect (Fig. 1B) was created using the surgical technique recently published by our group [17, 25, 26]. The animal ethics committee of the Queensland University of Technology approved the present study (animal ethics approval no. 1000000385). All animal surgeries were performed at the Queensland University of Technology Medical Engineering Research Facility (The Prince Charles Hospital, Chermside, Brisbane, Queensland, Australia). Three different treatment groups ($n = 8$ each) were used in the present study. In group I, the polycaprolactone-hydroxyapatite (PCL-HA) scaffold was implanted into the defect site only (Fig. 1C). In group II, the PCL-HA scaffold was combined with delayed injection of 100 million allogenic BMSCs 4 weeks after scaffold implantation (Fig. 1D–1F). In group III, the defect was filled with an autologous bone graft taken from the iliac crest of the sheep. Data from the latter group were obtained in previous studies (detailed results of study group III are given in [25]) and used as the reference standard comparison in the present study. All the sheep were euthanized at 12 months after surgery by intravenous injection of 60 mg/kg pentobarbital sodium (Lethabarb; Virbac Animal Health, Milperra, New South Wales, Australia, <http://www.virbac.com>). All reagents were purchased from Sigma-Aldrich unless stated otherwise (Sigma-Aldrich, Castle Hill, New South Wales, Australia, <http://www.sigmaaldrich.com/australia>).

Scaffold Design and Preparation

Biodegradable composite scaffolds (outer diameter 16 mm, height 30 mm, inner diameter 8 mm) composed of medical grade polycaprolactone (80% wt) and hydroxyapatite (20% wt) (mPCL-HA) were used in the present study. The scaffolds were produced by fused deposition modeling, as previously reported [17, 25]. To enhance the osteoinductive properties of the scaffold, the surface was coated with a layer of calcium phosphate (CaP) using a previously published protocol [28]. The scaffolds had a porosity of 74% and a 0/90° lay down pattern. This architectural layout is particularly suitable for load bearing applications, because the fully interconnected network can withstand early physiological and mechanical stress in a manner similar to that of cancellous bone. Moreover, the architectural pattern allows retention of coagulating blood during the early phase of healing and bone in-growth at later stages. Before surgery, all scaffolds were surface treated for 6 hours with 1 M NaOH to etch the surface, increasing the scaffold hydrophilicity to improve cell attachment, and washed 5 times with phosphate-buffered saline. Scaffold sterilization was achieved by incubation in 70% ethanol for 5 minutes and subsequent evaporation combined with UV irradiation for 30 minutes.

Before implantation, the scaffolds were modified by punching 3 holes on the back side of the scaffold (diameter 4 mm) and 4 smaller holes on the front side (diameter 3 mm) (Fig. 1A). The 4 holes in the front part of the scaffold were used to enable minimally invasive injection of the cells into the scaffold after 4 weeks and were placed along the axis of the plate. The holes on the back were placed in proximity to the blood vessels in the

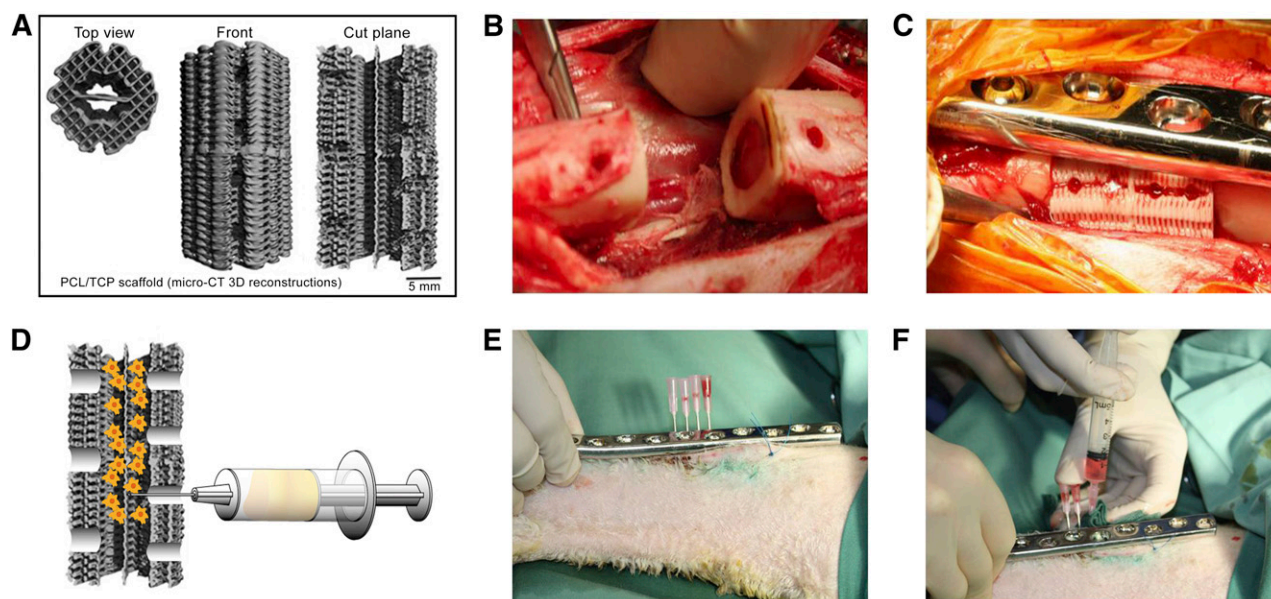


Figure 1. Scaffold design and surgical procedure. **(A):** Micro-CT 3D reconstruction of PCL-hydroxyapatite scaffold. **(B):** Posterior three holes placed in proximity to neurovascular bundle. **(C):** Surgical implantation in situ with four holes for delayed injection of bone marrow stromal cells (BMSCs) placed next to dynamic compression (DC) plate. **(D):** Schematic illustration of injection of BMSCs into the scaffold. **(E, F):** Minimally invasive percutaneous delayed BMSC injection procedure using another DC plate as a template to localize the injection holes and four separate needles to inject the cells into the scaffold. Abbreviations: 3D, three-dimensional; CT, computed tomography; PCL, polycaprolactone; TCP, tricalcium phosphate.

dorsal part of the bone defect to allow the ingrowth of new blood vessels (Fig. 1B, 1C).

Isolation and Differentiation of Allogenic BMSCs

Ovine BMSCs were obtained from Merino sheep that were not included in the present study (allogenic BMSCs). The BMSCs were obtained, cultured, and characterized with respect to surface marker profile and proliferation and differentiation potential, as previously reported in detail [29]. In brief, bone marrow aspirates were obtained from the iliac crest with the sheep under general anesthesia. The total bone marrow cell fraction ($5\text{--}15 \times 10^6$ cells per milliliter) was plated at a density of $10\text{--}20 \times 10^6$ cells per cm^2 in complete medium consisting of low-glucose Dulbecco's modified Eagle's medium (DMEM) supplemented with 10% fetal bovine serum (FBS), 100 U/ml penicillin, and 100 $\mu\text{g}/\text{ml}$ streptomycin (Sigma-Aldrich). The attached cells were passaged once and subsequently plated at a density of 10^3 cells per cm^2 to engineer the cell sheets. Two weeks before injection, the medium was changed to an osteogenic media (DMEM, 10% FBS, 100 U/ml penicillin, 100 $\mu\text{g}/\text{ml}$ streptomycin, 10 $\mu\text{l}/\text{ml}$ β -glycerol phosphate, 1 $\mu\text{l}/\text{ml}$ ascorbic acid, and 1 $\mu\text{l}/\text{ml}$ dexamethasone) to induce osteogenic differentiation. The mineralized extracellular matrices of the cell sheets were analyzed using alizarin red staining.

Delayed Injection Cell Delivery

Four weeks after implantation of the scaffolds, the allogenic BMSCs were injected percutaneously (Fig. 1). For this procedure, mineralized cell sheets containing 100×10^6 cells were detached from the cell culture flasks using a cell scraper and then fragmented with the pipette according to a previously described protocol [30, 31]. The cell sheet "solution" (4 ml) was then transferred equally to four 5-ml syringes under sterile conditions. The cell injection into the bone defects was performed with the sheep

under general anesthesia and sterile conditions in the operating room. The dynamic compression plate (DePuy Synthes, Sydney, New South Wales, Australia, <http://www.synthes.com>) was localized through the skin, and another identical plate was placed on top, over the skin, to identify the exact position of the plate holes (Fig. 1E). Four 14-gauge needles were placed into the 4 anterior scaffold holes percutaneously, and the BMSCs were injected (Fig. 1D, 1F).

Radiographic Analysis

Serial follow-up radiographs were taken at 3, 9, and 12 months after surgery to evaluate bone regeneration and determine the progression of bone bridging of the defect (Fig. 2). Conventional radiographic analysis (3.2 mA, 65 kV; Philips, Macquarie Park, New South Wales, Australia, <http://www.philips.com.au>) was performed in two standard planes (anteroposterior and mediolateral).

Biomechanical Testing

Before biomechanical testing, the fixation plates and screws were removed carefully from the experimental tibiae. Both tibial ends were embedded in Paladur (Heraeus Kulzer International, Hanau, Germany, <http://www.heraeus-kulzer.com>) dental acrylic and mounted in a biaxial testing machine (Instron 8874; Instron, Norwood, MA, <http://www.instron.com>) using a custom-made jig. Torsion testing was then conducted under angular displacement control at an angular velocity of $0.5^\circ/\text{s}$ and a constant compressive preload of 0.05 kN until the first signs of fracture occurred (Fig. 3). The maximum torsional moment (TM) and torsional stiffness (TS) were calculated and then normalized against the measured values of the contralateral, nonoperated tibia of the same sheep. Detailed protocols for biomechanical testing can be found in [25]. After biomechanical testing, right tibial samples were cut

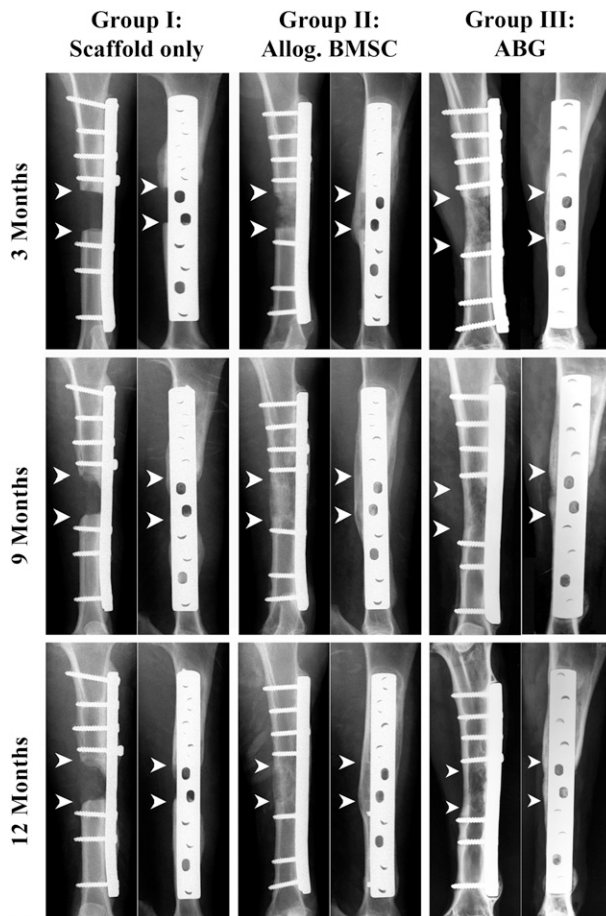


Figure 2. Representative clinical radiographic images at 3, 9, and 12 months after surgery. Defect reconstructed with polycaprolactone-hydroxyapatite (PCL-HA) scaffolds only (group I), PCL-HA scaffolds seeded with allogenic BMSCs (group II), and defects reconstructed with application of ABG (group III). Arrowheads indicate margins of bone defect. The images show radiographic signs of profound new bone formation and bridging of the defect site in the BMSC and ABG group. The scaffold-only group shows attenuated signs of new bone formation with no bridging of the defect site. Abbreviations: ABG, autologous bone graft; Allog., allogenic; BMSCs, bone marrow stromal cells.

to a length of 5 cm (3-cm defect site plus 1-cm of host bone on each end) for additional microcomputed tomography (micro-CT) scanning.

Micro-CT

After mechanical testing, micro-CT scans of the defect site were performed using the protocols recently published by our group [25]. All samples were imaged using a micro-CT 40 scanner (Scanco Medical AG, Bassersdorf, Switzerland, <http://www.scanco.ch>) to quantify the newly formed mineralized tissue. Specimens were placed in a sample tube and scanned at an energy of 70 kVp and intensity of 114 μ A, resulting in a voxel size of 18 μ m. The analyzed volume of interest included the defect region and adjacent host bone only. The total bone volume was measured for the complete defect volume, and the axial bone volume distribution was assessed by dividing the total length of the defect into three sections of equal length (proximal, middle, and distal; Fig. 4A).

Histology and Immunohistochemistry

All samples were fixed in 10% neutral buffered formalin for 1 week after completion of biomechanical testing and micro-CT analyses. For additional investigation, the samples were then sectioned in the transverse and sagittal planes; 2-mm-thick sagittal sections covering the full length of the defect area were cut from the middle of the specimen. Without decalcifying, these slides were embedded in methylmethacrylate resin (Technovit 9100 NEU; Heraeus Kulzer International), ground sectioned to 50 μ m, and stained with von Kossa/McNeal's tetrachrome to identify new bone formation and Goldner's trichrome to identify cellular details. The remaining parts were sectioned transversely into 3 areas (proximal, middle, distal) and decalcified in 15% EDTA for 6 months at 4°C. Next, the samples were embedded in paraffin, and 5- μ m-thick tissue slices were sectioned using a microtome (Leica RM 2265; Leica, Heerbrugg, Switzerland, <http://www.leica.com>). The slides were then deparaffinized with xylene and rehydrated before hematoxylin and eosin staining (Sigma-Aldrich) and mounting with Eukitt mountant (Sigma-Aldrich).

For immunohistochemical analysis, the slides were deparaffinized in xylene and rehydrated in decreasing concentrations of ethanol. Next, the sections were rinsed in distilled water and washed in 0.2 M Tris-HCl buffer (pH 7.4). Incubation with 3% H₂O₂ (diluted in 0.2 M Tris-HCl) for 30 minutes was used to block endogenous peroxidase activity. Next, the sections were washed 3 times in Tris buffer for 2 minutes each. Antigen retrieval was achieved by incubation with Proteinase K (Dako Australia, Botany, New South Wales, Australia, <http://www.dako.com>) for 20 minutes at room temperature. The slides were then washed with Tris buffer 3 times and incubated with 2% bovine serum albumin (Sigma-Aldrich) in a humidified chamber for 60 minutes. Next, the primary antibodies against the osteogenic markers collagen type I (Sapphire Bioscience, Waterloo, New South Wales, Australia, <http://www.sapphirebioscience.com>), osteocalcin (Sapphire Bioscience), and endothelium-related von Willebrand factor (Dako Australia, Campbellfield, Victoria, Australia) were applied and incubated at 4°C overnight. The sections were consecutively washed three times with Tris buffer and incubated with secondary antibody peroxidase-labeled dextran polymer conjugated according to immunoglobulins (DAKO EnVision+ Dual Link System Peroxidase, Dako) at room temperature in humidified chambers for 60 minutes. After another washing with Tris buffer 3 times for 2 minutes each, color development was performed using a liquid 3,3'-diaminobenzidine-based system (DAKO). The slides were then counterstained with hematoxylin for 5 minutes, followed by ammonium hydroxide 0.1% for 30 seconds and bluing under tap water. Next, Eukitt quick-hardening mounting medium (Sigma-Aldrich) was used for coverslip mounting of the dehydrated slides.

Scanning Electron Microscopy for Osteocytes in Mineralized Matrix

Resin-embedded samples received a mirror finish polish by sequential wet sanding with 400, 600, and 1,200 grit sandpaper and a final polish with 1.0 α aluminum powder using a soft cloth polishing wheel. The polished surfaces were then etched with 37% phosphoric acid for 2–10 seconds, washed in sodium hypochlorite bleach for 5 minutes, and then briefly rinsed in distilled water. After drying, the resin blocks were gold sputtered coated (Leica EM SCD005, Leica Microsystems Australia, North Ryde, New South Wales, Australia, <http://www.leica-microsystems.com>) and

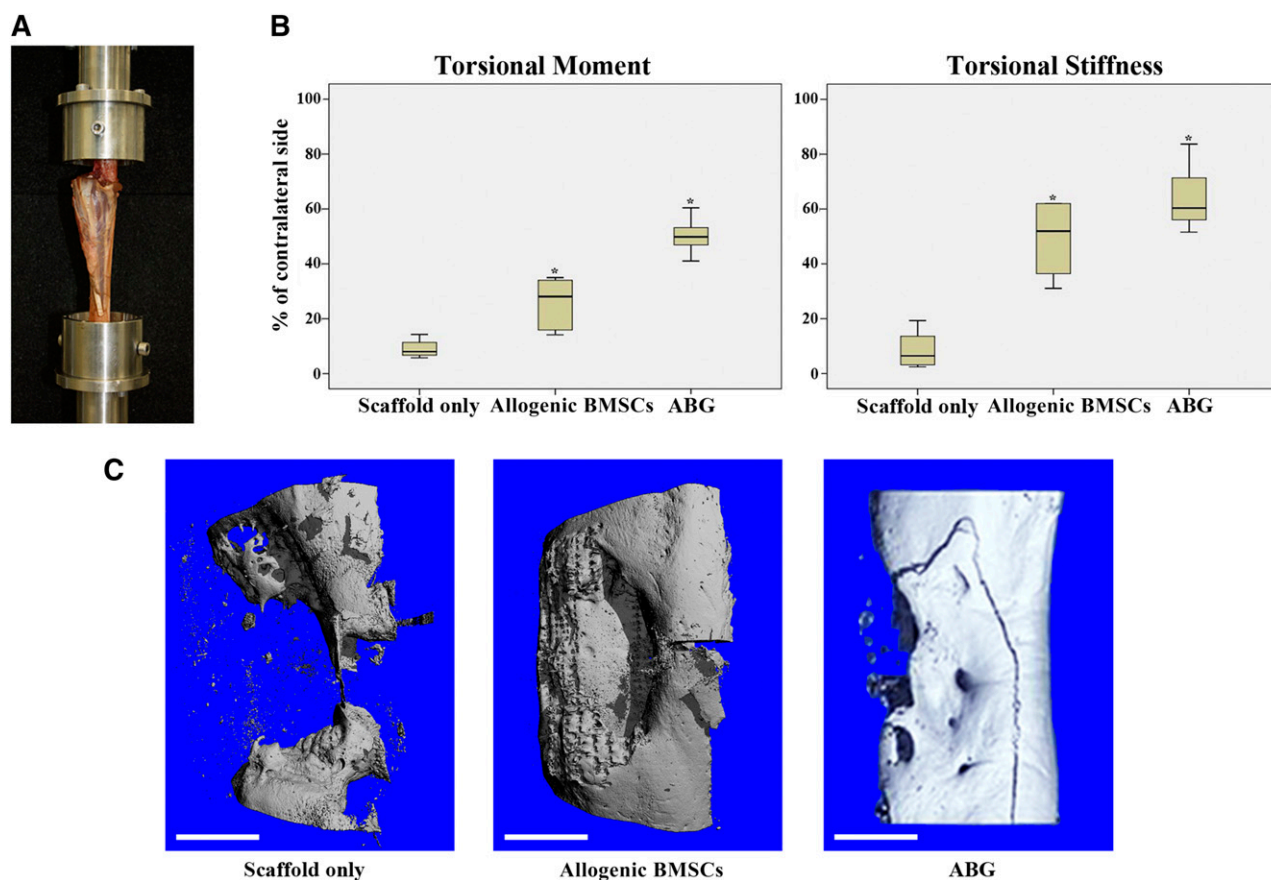


Figure 3. Biomechanical testing and microcomputed tomography (micro-CT) analysis. **(A):** Biomechanical testing was performed with both ends of the tibia embedded in methylmethacrylate with the tibial axis vertically aligned. **(B):** Results of biomechanical testing after 12 months for maximal torsional moment and torsional stiffness. Box plots demonstrate median values with first and third quartile in all experimental groups. Error bars represent maximum and minimum values. Asterisks indicate statistical significance ($p < .05$). **(C):** Representative three-dimensional reconstructions of micro-CT scans (proximal bone end facing upward) for scaffold-only group, allogenic BMSC group, and ABG group. Fracture line visible resulted from biomechanical testing (torsion until failure) before micro-CT analysis. Scale bars = 1 cm **(C)**. Abbreviations: ABG, autologous bone graft; BMSC, bone marrow stromal cell.

examined using an FEI Quanta 200 environmental scanning electron microscope (FEI, Hillsboro, OR, <http://www.fei.com>) operating at 10 kV.

Statistical Analysis

Statistical analysis was performed using a two-tailed Mann-Whitney U test (SPSS, version 18.0; IBM Corp., Armonk, NY, <http://www.ibm.com>). The P values were adjusted according to Bonferroni-Holm; $P < .05$ was considered statistically significant.

RESULTS

Surgical Procedure and Postoperative Follow-Up

All 24 sheep ($n = 8$ sheep per group) tolerated the surgical procedure well, and no postoperative infections or other complications were observed. All the sheep were in good health and survived the experimental period, gaining weight in the months after surgery. In particular, no clinical signs were seen of an immune response or implant rejection to the injected allogenic cells. Venous blood samples taken preoperatively and on days 1, 3, 7, 14, and 21 postoperatively from all the sheep indicated no signs of graft rejection.

Culture and Differentiation of Allogenic BMSCs

Bone marrow stromal cells (allogenic BMSCs) were obtained, cultured, and characterized with respect to the surface marker profile and proliferation and differentiation potential as previously reported in detail [29]. In brief, BMSCs were isolated from bone marrow aspirations, as previously described [21]. Total bone marrow cells were plated at a density of $1-2 \times 10^7$ cells per cm^2 in DMEM and cultured until they were confluent. Two weeks before implantation, the medium was changed to an osteogenic media to induce osteogenic differentiation [29]. Within a few days, the cells showed a clear response to the osteogenic induction media with a pronounced morphological change from an elongated shape to a compact cobblestone-like appearance. The potential of BMSCs to secrete a mineralized extracellular matrix was analyzed via histologic and immunocytochemistry examination. After 2 weeks of induction, the cultures were shown to produce a collagen type I-rich extracellular matrix with extensive amounts of alizarin red-positive mineral deposits throughout the adherent layers.

Radiographic Analysis

Correct positioning of the scaffold, plate, and screws was radiographically confirmed immediately after surgery. At 3 months

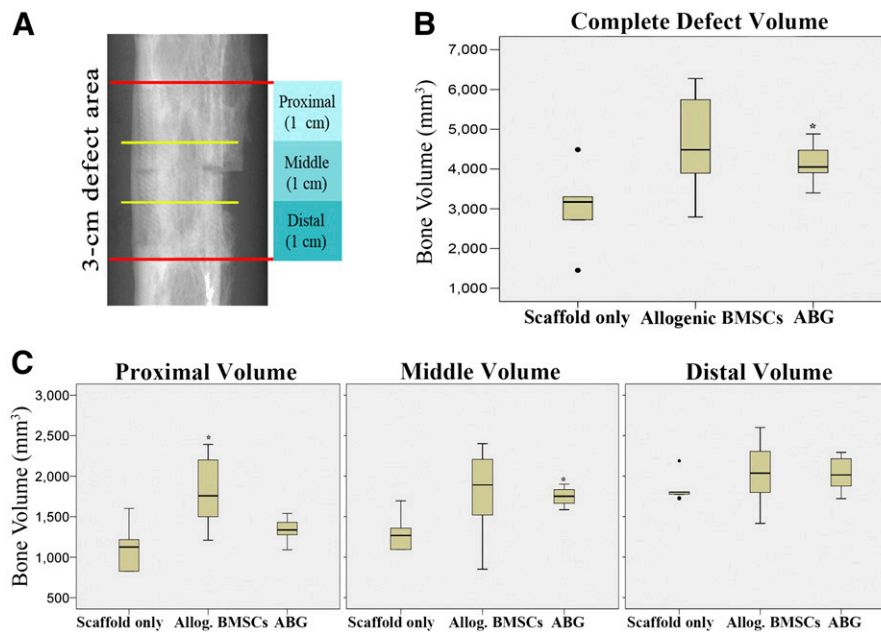


Figure 4. Microcomputed tomography analysis at 12 months after surgery. **(A):** Image illustrating three different areas of interest. **(B):** Total bone volume in complete defect area. **(C):** Bone volume results in different areas of interest. Box plot demonstrating median amounts of newly formed bone with first and third quartile within the 3-cm defects 12 month after surgery. Error bars represent maximum and minimum values. Abbreviations: ABG, autologous bone graft; Allog., allogenic; BMSC, bone marrow stromal cell.

after surgery, bone formation was observed in the allogenic BMSC group originating from the dorsal part of the tibia where the defect is covered by the large muscle of the lower leg. The scaffold-only group showed minor bone formation within the defect; in 1 sheep loosening of 1 screw was observed without additional signs of implant loosening or failure. The radiographic analysis after 9 months revealed no movement of the scaffolds or implants and increased bone formation was observed in the ABG group and allogenic BMSC group. In contrast, the scaffold-only group showed only minimal signs of new bone formation. After 12 months, no additional implant loosening was observed in any sheep. Complete bony bridging of the defects had occurred in all autograft and allogenic BMSC sheep (groups II and III; Fig. 2). In group I (PCL scaffold only), no sheep showed defect bridging, and only minor bone formation was observed within the defect site (Fig. 2).

Biomechanical Analysis

Biomechanical testing was performed on all specimens after euthanasia of the sheep at 12 months postoperatively (Fig. 3A). All experimental results were compared with the results from the corresponding contralateral, nonoperated tibia. Biomechanical testing revealed significantly higher values for the maximal TM of the ABG group than for the allogenic BMSC and scaffold-only groups ($p = .002$ and $p = .002$, respectively). Furthermore, the allogenic BMSC group showed significantly higher values compared with the scaffold-only group ($p = .003$). The TS for the ABG group and allogenic BMSC group was significantly higher than that for the scaffold-only group ($p = .002$ and $p = .003$, respectively). However, no statistically significant differences were found between the ABG group and allogenic BMSC group for TS ($p = .298$; Fig. 3B).

Micro-CT Analysis

Micro-CT analysis confirmed the trend from the clinical radiographic analysis regarding union rates and the amount of new bone formation. In three-dimensional reconstructions of mineralized tissue in the defect volume (Fig. 3C), the defect was shown to remain unbridged in the scaffold-only group (supplemental online Video 2). In contrast, the BMSC and ABG groups showed large amounts of new bone formation with complete bridging of the defect (a representative three-dimensional reconstruction of mineralized tissue in the BMSC group is given in supplemental online Video 3). When analyzing the total bone volume (the bone volume over the complete defect size), the mean values of newly formed bone in the BMSC group were slightly higher than those in the ABG group, but without significant differences ($p = .284$; Fig. 4B). In both the ABG and the BMSC group, the total bone volume was significantly higher than that in the scaffold-only group ($p = .04$ and $p = .047$, respectively). Dividing the bone defect into three areas of interest (proximal, middle, distal; Fig. 4A), the BMSC group showed significantly more bone formation in the proximal part of the defect compared with the ABG group and scaffold-only group ($p = .016$ and $p = .019$, respectively). Furthermore, the ABG group showed significantly more bone formation compared with the scaffold-only group for the whole defect and for the middle regions of interest ($p = .04$ and $p = .013$, respectively). No significant differences among the groups were found in the distal defect area (Fig. 4C).

Histology and Immunohistochemistry

In accordance with the imaging results from conventional radiographs and micro-CT, the histological analysis showed profound new bone formation in the defect area in and around the scaffold for the allogenic BMSC group, with complete bony bridging of the defect site in almost all the sheep. In contrast,

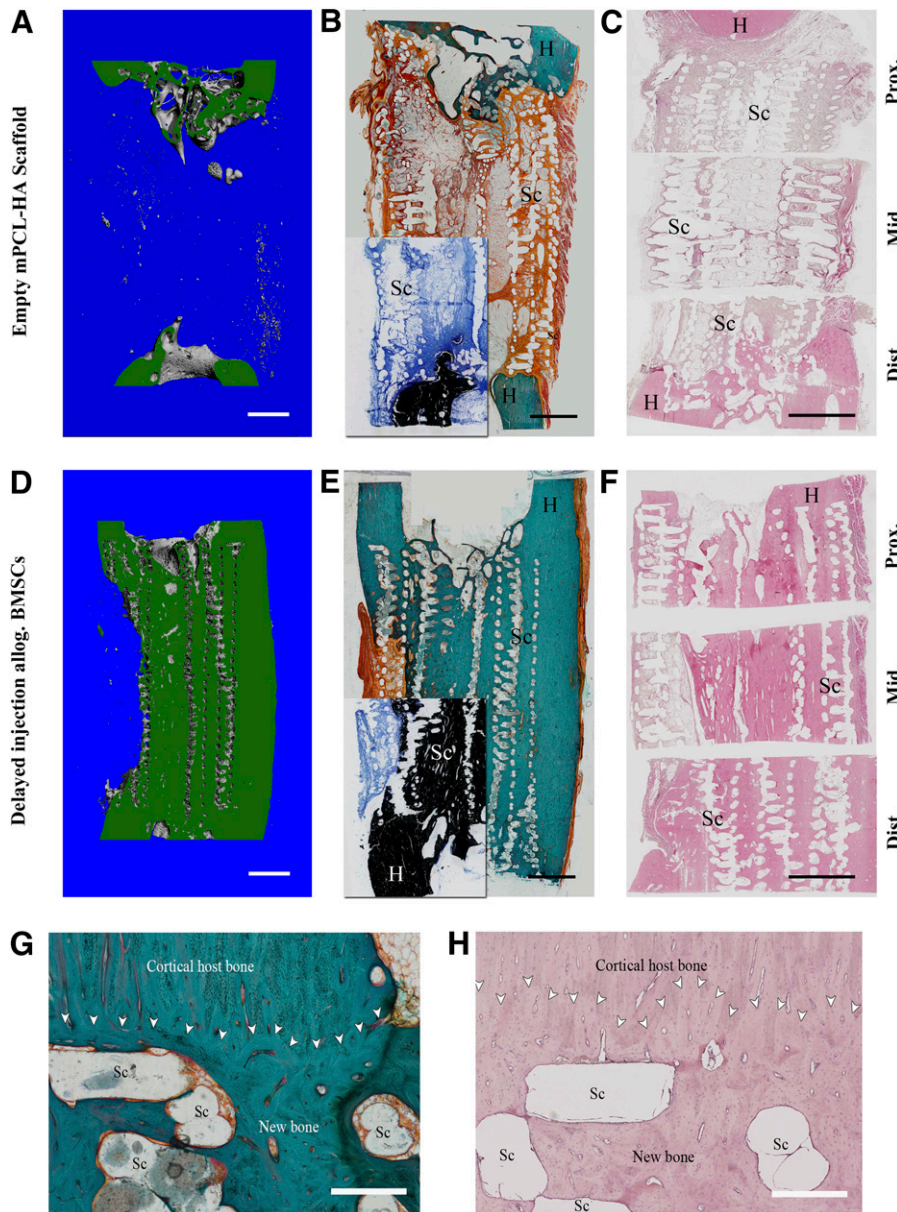


Figure 5. Representative images of histological staining for the empty scaffold group (A–C) and the allogenic BMSC group (D–H). Corresponding longitudinal sections (in green) through the three-dimensional reconstruction of mineralized tissue within the defect from microcomputed tomography data (A, D) are shown for comparison. Goldner’s trichrome stain (B, E) showed significant amount of new bone formation in the allogenic BMSC group compared with the empty scaffold group. Von Kossa/McNeal stain (insets in [B] and [E]) of corresponding areas confirm formation of mineralized tissue. Hematoxylin and eosin staining (C, F) also showed formation of new bone attenuated on scaffold-only group. Scaffold appears as a void owing to dissolution of PCL by xylene during processing. (G, H): Detailed view of host bone-scaffold interface of representative sample from allogenic BMSC group; Goldner’s trichrome stain (G) and hematoxylin and eosin stain (H). Good osteointegration of the scaffold and good bonding of the newly formed bone tissue with the host bone is visible. Scaffold struts appear as void owing to dissolving of PCL-HA by xylene during preparation. White arrowheads indicate interface between new bone/scaffold and host bone. Scale bars = 5 mm (A–F) and 500 μm (G, H). Abbreviations: Allog., allogenic; BMSC, bone marrow stromal cell; H, host bone; mPCL-HA, medical grade polycaprolactone-hydroxyapatite; Mid., middle; Prox., proximal; Sc, scaffold struts.

the empty PCL-HA scaffold-only group showed minor formation of new mineralized tissue and a high percentage of fibrous tissue/fat tissue in the defect area around and within the scaffold. The results of Goldner’s trichrome, Von Kossa/McNeal, and hematoxylin and eosin staining are shown in Figure 5, with the corresponding cut planes of three-dimensional reconstructions from micro-CT analyses.

Histological analysis of the scaffold-host bone interface showed good integration of the PCL-HA scaffold in the

allogenic BMSC group, with good bonding of the newly formed bone to the host bone. The results also showed good osteointegration of the PCL-HA scaffold, with newly formed bone tissue in the defect area itself (Fig. 5G, 5H). The scaffold-only group also displayed good integration of the scaffold/newly formed bone with the host bone at the defect margins. However, owing to the limited formation of total new bone volume in this group, comprehensive assessment of osteointegration was restricted.

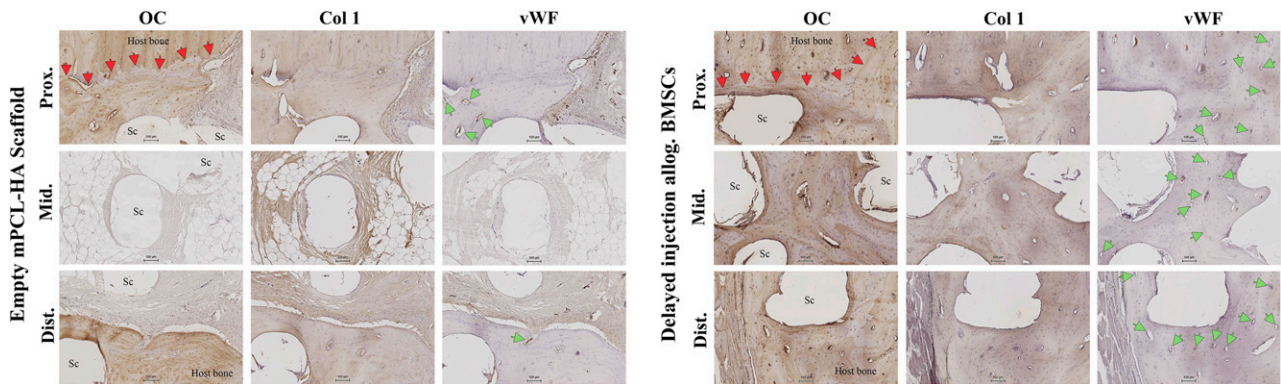


Figure 6. Representative images of immunohistochemical analysis using antibodies against OC, Col 1, and vWF. Red arrowheads indicate host bone–new bone/scaffold interface; green arrowheads indicate vasculature. Early osteogenic marker Col 1 was found in newly formed bone of all segments of the allogenic BMSC group and newly formed bone proximally and distally and in fibrous tissue in the defect middle for the scaffold-only group. Late osteogenic marker OC was found in tissue-engineered bone in all segments in the allogenic BMSC group but only at the proximal and distal host bone–scaffold interfaces in the scaffold-only group. Profound neovascularization of the new bone tissue in all segments was present in the allogenic BMSC group (green arrowheads indicate blood vessels stained positively for vWF in new bone). Scaffold-only group showed new blood vessels in the proximal and distal interface areas. Scale bars = 100 μ m. Abbreviations: Allog., allogenic; BMSC, bone marrow stromal cell; Col 1, collagen 1; Dist., distal; Mid., middle; mPCL-HA, medical grade polycaprolactone-hydroxyapatite; OC, osteocalcin; Prox., proximal; Sc, scaffold struts; vWF, von Willebrand factor.

Immunohistochemical analysis (Fig. 6) showed collagen type I to be present in newly formed bone tissues of the allogenic BMSC group in all three areas (proximal, middle, and distal). For the scaffold-only group, collagen type I was present in newly formed bone at the scaffold–host bone interface in the proximal and distal segments. Collagen type I was also found in the fibrous tissue of the nonbridged defect site in this group, predominantly around the scaffold struts. Osteocalcin (OC) is a noncollagenous, vitamin K-dependent protein secreted in the late stage of osteoblast differentiation regulating bone mineralization and osteoblast and osteoclast activity [32]. Newly formed bone tissue in all three segments of the defect revealed positive immunohistochemical staining for OC in the allogenic BMSC group. These results indicate additional maturation of the newly formed bone and matrix mineralization in the allogenic BMSC group. Furthermore, OC was highly expressed around the scaffold struts. The scaffold-only group had OC present in limited areas of the host bone–scaffold interface at the proximal and distal end of the defect, indicating some degree of bone remodeling in these areas. However, no OC was detected in the middle segments of the defect site (only the early osteogenic marker collagen type I was identified). Endothelial-related Von Willebrand factor (vWF), used as a marker for vasculature, was present in the newly formed bone of all segments in the allogenic BMSC group, indicating neovascularization of the tissue-engineered bone. In the empty scaffold group, vWF was also found in the newly formed bone of the proximal and distal interfaces. The histological and immunohistochemical results for the autologous bone graft group have been previously published and are not shown in the present study [25, 33].

Scanning Electron Microscopy Imaging

Scanning electron microscopy (SEM) in back scattered electron mode was used to further investigate the ultrastructural properties of the tissue engineered bone and its interactions with the host bone and CaP-coated scaffold surface for the allogenic BMSC group (Fig. 7). In accordance with the histological and immunohistochemical results, SEM imaging showed good

integration of the newly formed bone with the host bone and the scaffold interface (Fig. 7A–7D). Furthermore, SEM imaging indicated the presence of a complex and mature (large vessel diameter, multiple branches) vascular network in the newly formed bone (Fig. 7E, 7F).

DISCUSSION

Cell-based therapies are promising strategies in regenerative medicine. However, future strategies will certainly be influenced by the cell source used: either allogenic or autologous cells and the donor site of the cells.

A number of issues need to be considered comparing the efficiency and efficacy when considering allogenic and autologous cells for scaffold cell-based bone engineering strategies. The treatment of large segmental bone defects requires a large number of cells with a high osteogenic differentiation potential. If using an autologous cell source, the cost and the time consideration in harvesting and culturing the cells is high. Therefore, the use of an allogenic cell source, which can be used as an “off-the-shelf product” and that would enable a high number of cells to be attained within an acceptable time frame for the treatment of traumatic bone defects, is preferable. The major disadvantage of using allogenic cell sources is the possible risk of an immune reaction. For more details, the reader is referred to a comprehensive review of the advantages and disadvantages of autologous and allogenic cells for regenerative medicine by Mason and Dunhill [34].

We have recently shown allogenic MSCs cultured for 4 weeks in a PCL-HA scaffold can be safely transplanted in a 3-cm, critical-sized tibial defect in an ovine animal model, and no clinical signs of an immunological reaction to allogenic cells could be detected [21]. However, the bone regeneration capacity of such a TEC is much lower than that of an autograft and/or a scaffold loaded with bone morphogenetic protein 7 [25].

The immunological results published in the present study confirm the results from our previous study [21] in which we implanted scaffold/cell constructs into a freshly created 3-cm

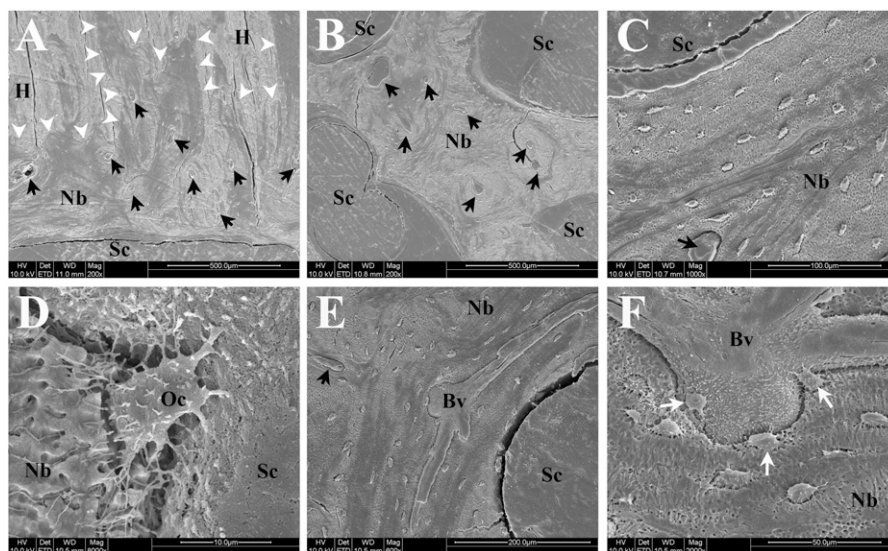


Figure 7. Representative scanning electron microscopic images of newly formed bone and interfaces with scaffold/host bone in the delayed injection bone marrow stromal cell group. Black arrows indicate blood vessels within newly formed bone. **(A):** Interface of newly formed bone with host bone and scaffold showing excellent osteointegration (white arrowheads indicate host bone-new bone interface). **(B):** Osteointegration of newly formed bone with scaffold in the middle of the defect. **(C):** Higher magnification image showing integration between scaffold strut and tissue-engineered bone. **(D):** High-resolution image of an osteocyte partly embedded in newly formed bone matrix and also directly attaching to rough surface of scaffold strut (calcium-phosphate coating). **(E):** Image of large mature blood vessel with multiple branches inside tissue-engineered bone. **(F):** High-resolution image of blood vessels shown in **(E)** depicting close proximity and interaction of osteocytes (white arrows) to/with blood vessel. Fissures visible in images are artifacts resulting from preparation process of specimen. Abbreviations: Bv, blood vessel; H, host bone; Nb, newly formed bone; Oc, osteocyte; Sc, scaffold struts.

tibial defect in that the delayed application of allogenic cells did not cause any clinical signs of an immune reaction and can be therefore defined as a safe procedure.

Most importantly, our results demonstrate the significant difference of a delayed injection of allogenic bone marrow-derived MSCs (BMSCs) by directly comparing the results to different scaffold-based bone regeneration procedures. This, to the best of our knowledge, is the first reported cell-based technique that led to significant bone regeneration with complete bridging in a critically sized segmental defect in a large preclinical animal model. The results from biomechanical testing, radiographs, and micro-CT in the allogenic BMSC group were comparable to the results from the current reference standard of an autologous bone graft and were significantly enhanced compared with the previously published data set [21], in which we applied a classic tissue engineering approach by implanting a scaffold/cell construct into a freshly created bone defect. This indicates that the delayed injection strategy, combined with an osteoconductive composite scaffold, is not only superior to a directly implanted scaffold/cell construct but also provides the efficacy to be a relevant alternative to the use of ABGs in the treatment of large segmental bone defects.

However, to study the survival and proliferation of the transplanted cells embedded in the injected cell sheet, a suitable and reliable cell labeling method that would allow the tracking of the cells for several months in a large preclinical animal model should be developed and validated in additional experiments. In classic tissue engineering concepts, confluent cultured cells are usually harvested by enzymatic digestion before seeding onto a scaffold. The use of enzymatic digestion in cell culture is a standard procedure and well accepted; however, this method destroys the extracellular matrix (ECM) produced after osteogenic differentiation. The ECM is rich in

growth factors and has strong osteogenic potential. Hence, our work built on the results from the Okano group, which was among the first to use the benefits of cell sheet technologies to allow cells to be recovered within their own matrix after transplantation [35].

The concept of delayed injection of MSCs has been shown to have beneficial effects in the experimental treatment of diabetic renal injuries in rats [36] and maxilla defects in goats [37]. Our results so far indicate that the concept of delayed injection of allogenic BMSCs is beneficial in long bone defects. Moving forward, additional work must investigate this concept further to optimize delayed cell injection and identify the optimal time point for cell transplantation and the optimal cell dosage to achieve the best possible bone regeneration according to the defect size and location.

In the present study, the concept of delayed injection of cells for tissue engineering approaches has been demonstrated to be a capable technique for bone regeneration that could lead to improved outcomes of cell-based tissue engineering approaches in the future. Successful translation of delayed allogenic cell transplantation into routine practice could provide clinicians with beneficial treatment alternatives to autologous bone grafting for challenging bone defects that circumvents the associated morbidity and cost implications associated with autografting. Furthermore, the concept of delayed injection of cells for tissue engineering approaches could be used in other areas of regenerative medicine and might lead to improvements in universal cell-based tissue engineering strategies.

ACKNOWLEDGMENTS

We thank Siamak Saifzadeh, Mostyn Yong, and Brendan Jones for assistance with the surgical procedures. We thank the staff at the Queensland University of Technology Medical Engineering

Research Facility for assistance and administrative and technical support. We thank the Queensland University of Technology (QUT) Bone Tissue Morphology Group and QUT Histology Facility for helping with the preparation of the histological specimens and Christina Theodoropoulos for the preparation of the scanning electron microscopic images. A part of this work was supported by funding through the National Health and Medical Research Council (Grant 1055575), the Australian Research Council (Dr. Hutmacher's ARC Future Fellowship and ARC Linkage Grant LP130100945), the Wesley Foundation (Grant 2012-03), and the German Research Foundation (Grants BE 4492/1-2 and HE 7074/1-1).

AUTHOR CONTRIBUTIONS

A.B., J.H., and D.W.H.: design and performance of experiments, data analysis, manuscript writing; M.A.W., R.S., and M.N.: provision of analytical tools, data analysis, histological result analysis; M.A.S. and M.N.: translational and clinical viewpoint input; D.W.H.: study supervision.

DISCLOSURE OF POTENTIAL CONFLICTS OF INTEREST

The authors indicated no potential conflicts of interest.

REFERENCES

- Xu XQ, Sun W. Perspective from the heart: the potential of human pluripotent stem cell-derived cardiomyocytes. *J Cell Biochem* 2013; 114:39–46.
- Vono R, Spinetti G, Gubernator M et al. What's new in regenerative medicine: Split up of the mesenchymal stem cell family promises new hope for cardiovascular repair. *J Cardiovasc Transl Res* 2012;5:689–699.
- Domínguez-Bendala J, Lanzoni G, Inverardi L et al. Concise review: Mesenchymal stem cells for diabetes. *STEM CELLS TRANSLATIONAL MEDICINE* 2012;1:59–63.
- Jackson WM, Nesti LJ, Tuan RS. Concise review: Clinical translation of wound healing therapies based on mesenchymal stem cells. *STEM CELLS TRANSLATIONAL MEDICINE* 2012;1:44–50.
- Bernardo ME, Fibbe WE. Safety and efficacy of mesenchymal stromal cell therapy in autoimmune disorders. *Ann NY Acad Sci* 2012; 1266:107–117.
- Honmou O, Onodera R, Sasaki M et al. Mesenchymal stem cells: Therapeutic outlook for stroke. *Trends Mol Med* 2012;18:292–297.
- Bonab MM, Sahraian MA, Aghsaie A et al. Autologous mesenchymal stem cell therapy in progressive multiple sclerosis: An open label study. *Curr Stem Cell Res Ther* 2012;7:407–414.
- D'Agostino B, Sullo N, Siniscalco D et al. Mesenchymal stem cell therapy for the treatment of chronic obstructive pulmonary disease. *Expert Opin Biol Ther* 2010;10:681–687.
- Roemeling-van Rhijn M, Weimar W, Hoogduijn MJ. Mesenchymal stem cells: Application for solid-organ transplantation. *Curr Opin Organ Transplant* 2012;17:55–62.
- Maumus M, Guérit D, Toupet K et al. Mesenchymal stem cell-based therapies in regenerative medicine: Applications in rheumatology. *Stem Cell Res Ther* 2011;2:14.
- Bernardo ME, Pagliara D, Locatelli F. Mesenchymal stromal cell therapy: A revolution in regenerative medicine? *Bone Marrow Transplant* 2012;47:164–171.
- Kuroda Y, Kitada M, Wakao S et al. Bone marrow mesenchymal cells: How do they contribute to tissue repair and are they really stem cells? *Arch Immunol Ther Exp (Warsz)* 2011;59: 369–378.
- Ren G, Chen X, Dong F et al. Concise review: Mesenchymal stem cells and translational medicine: Emerging issues. *STEM CELLS TRANSLATIONAL MEDICINE* 2012;1:51–58.
- Si YL, Zhao YL, Hao HJ et al. MSCs: Biological characteristics, clinical applications and their outstanding concerns. *Ageing Res Rev* 2011; 10:93–103.
- Kon E, Filardo G, Roffi A et al. Bone regeneration with mesenchymal stem cells. *Clin Cases Miner Bone Metab* 2012;9:24–27.
- Shekkeris AS, Jaiswal PK, Khan WS. Clinical applications of mesenchymal stem cells in the treatment of fracture non-union and bone defects. *Curr Stem Cell Res Ther* 2012;7:127–133.
- Berner A, Reichert JC, Müller MB et al. Treatment of long bone defects and non-unions: From research to clinical practice. *Cell Tissue Res* 2012;347:501–519.
- Smith JO, Aarvold T, Tayton ER et al. Skeletal tissue regeneration: Current approaches, challenges, and novel reconstructive strategies for an aging population. *Tissue Eng Part B Rev* 2011;17:307–320.
- El Tamer MK, Reis RL. Progenitor and stem cells for bone and cartilage regeneration. *J Tissue Eng Regen Med* 2009;3:327–337.
- Kagami H, Agata H, Tojo A. Bone marrow stromal cells (bone marrow-derived multipotent mesenchymal stromal cells) for bone tissue engineering: Basic science to clinical translation. *Int J Biochem Cell Biol* 2011;43:286–289.
- Berner A, Reichert JC, Woodruff MA et al. Autologous vs. allogenic mesenchymal progenitor cells for the reconstruction of critical sized segmental tibial bone defects in aged sheep. *Acta Biomater* 2013;9:7874–7884.
- Marsell R, Einhorn TA. The biology of fracture healing. *Injury* 2011;42:551–555.
- Lienemann PS, Lutolf MP, Ehrbar M. Biomimetic hydrogels for controlled biomolecule delivery to augment bone regeneration. *Adv Drug Deliv Rev* 2012;64:1078–1089.
- Claes L, Recknagel S, Ignatius A. Fracture healing under healthy and inflammatory conditions. *Nat Rev Rheumatol* 2012;8:133–143.
- Reichert JC, Cipitria A, Epari DR, et al. A tissue engineering solution for segmental defect regeneration in load-bearing long bones. *Sci Transl Med* 2012;4:141ra93.
- Reichert JC, Saifzadeh S, Wullschlegler ME et al. The challenge of establishing preclinical models for segmental bone defect research. *Biomaterials* 2009;30:2149–2163.
- Reichert JC, Epari DR, Wullschlegler ME et al. Establishment of a preclinical ovine model for tibial segmental bone defect repair by applying bone tissue engineering strategies. *Tissue Eng Part B Rev* 2010;16:93–104.
- Berner A, Boerckel JD, Saifzadeh S et al. Biomimetic tubular nanofiber mesh and platelet rich plasma-mediated delivery of BMP-7 for large bone defect regeneration. *Cell Tissue Res* 2012;347:603–612.
- Reichert JC, Gohlke J, Friis TE et al. Mesodermal and neural crest derived ovine tibial and mandibular osteoblasts display distinct molecular differences. *Gene* 2013;525:99–106.
- Hesami P, Holzappel BM, Taubenberger A et al. A humanized tissue-engineered in vivo model to dissect interactions between human prostate cancer cells and human bone. *Clin Exp Metastasis* 2014;31:435–446.
- Zhou Y, Chen F, Ho ST et al. Combined marrow stromal cell-sheet techniques and high-strength biodegradable composite scaffolds for engineered functional bone grafts. *Biomaterials* 2007;28:814–824.
- Neve A, Corrado A, Cantatore FP. Osteocalcin: Skeletal and extra-skeletal effects. *J Cell Physiol* 2013;228:1149–1153.
- Reichert JC, Epari DR, Wullschlegler ME et al. [Bone tissue engineering. Reconstruction of critical sized segmental bone defects in the ovine tibia]. *Orthopade* 2012;41:280–287.
- Mason C, Dunnill P. Assessing the value of autologous and allogeneic cells for regenerative medicine. *Regen Med* 2009;4: 835–853.
- Pirracco RP, Obokata H, Iwata T et al. Development of osteogenic cell sheets for bone tissue engineering applications. *Tissue Eng Part A* 2011;17:1507–1515.
- Park JH, Park J, Hwang SH et al. Delayed treatment with human umbilical cord blood-derived stem cells attenuates diabetic renal injury. *Transplant Proc* 2012;44:1123–1126.
- Meijer GJ, de Bruijn JD, Koole R et al. Cell-based bone tissue engineering. *PLoS Med* 2007;4:e9.



See www.StemCellsTM.com for supporting information available online.

Delayed Minimally Invasive Injection of Allogenic Bone Marrow Stromal Cell Sheets Regenerates Large Bone Defects in an Ovine Preclinical Animal Model

Arne Berner, Jan Henkel, Maria A. Woodruff, Roland Steck, Michael Nerlich,
Michael A. Schuetz and Dietmar W. Hutmacher

Stem Cells Trans Med published online April 1, 2015

The online version of this article, along with updated information and services, is
located on the World Wide Web at:

<http://stemcellstm.alphamedpress.org/content/early/2015/03/31/sctm.2014-0244>